Coupling design for a long-term anticipating synchronization of chaos

Kestutis Pyragas[1,2] and Tatjana Pyragienė[1]
[1]*Semiconductor Physics Institute, A. Goštauto 11, LT-01108 Vilnius, Lithuania*
[2]*Department of Theoretical Physics, Faculty of Physics, Vilnius University, LT-10222 Vilnius, Lithuania*
(Received 28 July 2008; published 27 October 2008)

We propose an algorithm of coupling design for a long-term anticipating synchronization of chaos and demonstrate its efficacy for typical chaotic systems: namely, the Rössler system, the double-scroll Chua circuit, and the Lorenz system. The maximum prediction time attained with our algorithm is several times larger than with the diagonal coupling usually used in the literature.

DOI: 10.1103/PhysRevE.78.046217 PACS number(s): 05.45.Xt, 02.30.Ks

Synchronization of oscillations is a phenomenon common to a large variety of nonlinear dynamical systems in physics, chemistry, and biology [1,2]. Whereas the first investigation on the synchronization phenomenon goes back to the work by Huygens in 1665, the past decades have witnessed a considerable interest in the topic of synchronization of chaotic systems. The behavior of chaotic systems is characterized by instability and, as the result, limited predictability in time. Intuitively it would seem that chaos and synchronization are two mutually exclusive notions. However, it has been shown that synchronization can appear in chaotic systems in many different ways, including identical [3,4], generalized [5], phase [6], projective [7], lag [8], and anticipating [9] synchronization. The latter type of synchronization introduced by Voss [9] some years ago is most counterintuitive.

In the case of anticipating synchronization one deals with two systems, a "master" and a "slave," which are coupled unidirectionally via a time-delay feedback in such a manner that the slave system predicts the behavior of the master system. More specifically, the coupling scheme introduced by Voss is as follows:

$$\dot{\mathbf{r}}_1 = \mathbf{f}(\mathbf{r}_1), \tag{1a}$$

$$\dot{\mathbf{r}}_2 = \mathbf{f}(\mathbf{r}_2) + \mathbf{K}[\mathbf{r}_1 - \mathbf{r}_2(t-\tau)], \tag{1b}$$

where $\mathbf{r}_1(t)$ and $\mathbf{r}_2(t)$ are the dynamic vector variables of the master and slave systems, respectively, $\mathbf{f}$ is a nonlinear vector function, τ is a delay time, and $\mathbf{K}$ is a coupling matrix. It is easy to see that the anticipatory synchronization manifold $\mathbf{r}_2(t)=\mathbf{r}_1(t+\tau)$ is a solution of Eqs. (1). For an appropriate choice of τ and $\mathbf{K}$ this solution can be stable; i.e., the slave anticipates by an amount τ the output of the master. This phenomenon has been studied numerically for a variety of systems [10–12] and justified experimentally in electronic circuits [13] and chaotic semiconductor lasers [14,15]. It has been also observed in excitable systems driven by random forcing [16,17].

Implementation of anticipating synchronization as a strategy for real-time forecasting of a given dynamics requires a design of coupling schemes with a possibly large anticipation time. The analysis performed in Ref. [9] shows that the scheme (1) with a diagonal matrix $\mathbf{K}$ is ineffective. Its maximum stably anticipation time is much shorter than the characteristic time scales of the system's dynamics. In order to enlarge the prediction time it was proposed to extend Eq. (1b) with a chain of N unidirectionally coupled slave systems [18]:

$$\dot{\mathbf{r}}_i = \mathbf{f}(\mathbf{r}_i) + \mathbf{K}[\mathbf{r}_{i-1} - \mathbf{r}_i(t-\tau)], \quad i = 2, \ldots, N+1. \tag{2}$$

Formally, the prediction time of this scheme is N times larger as compared to the scheme (1b). However, it was shown that the chain (2) is unstable to propagating perturbations and this convectivelike instability limits the number of slaves in the chain which can operate in a stable regime [19].

In this paper, we address the question whether is it possible to considerably prolong the prediction time via a suitable choice of the coupling matrix $\mathbf{K}$. For typical low-dimensional chaotic systems we give a positive answer. We propose an algorithm of design $\mathbf{K}$ and show that the prediction time can be enlarged several times in comparison to the diagonal coupling usually used in the literature. Utilizing the scheme (1) with the single-slave system we obtain a stably anticipation time comparable to the characteristic period of chaotic oscillations.

First we demonstrate a heuristic idea of our algorithm with the Rössler system [20], which is given by a three-dimensional (3D) vector variable $\mathbf{r}=[x,y,z]$ and vector field

$$\mathbf{f}(\mathbf{r}) = [-y-z, x+ay, b+z(x-c)]. \tag{3}$$

In the following we set $a=0.15$, $b=0.2$, and $c=10$ and suppose that both $\mathbf{r}$ and $\mathbf{f}$ are the vector columns. Although the Rössler system has two fixed points, the strange attractor originates from one of them, $\mathbf{r}_0=[(c-s)/2,(s-c)/2a, (c-s)/2a]$, located close to the origin, where $s=(c^2-4ab)^{1/2}$. The fixed point is a saddle focus with an unstable 2D manifold (an unstable spiral) almost coinciding with the (x,y) plane and a stable 1D manifold almost coinciding with the z axis. The phase point of the system spends most time in the (x,y) plane moving along the unstable spiral according to the approximate equations $\dot{x}=-y$ and $\dot{y}=x+ay$. Whenever x approaches a value $x\approx c$, the z variable comes into play. The phase point leaves for a short time the (x,y) plane and then returns to the origin via a stable z-axis manifold.

Taking into account such a topology of the strange attractor we choose the coupling matrix as $\mathbf{K}=k\mathbf{Q}$, where k is a scalar parameter defining the coupling strength and

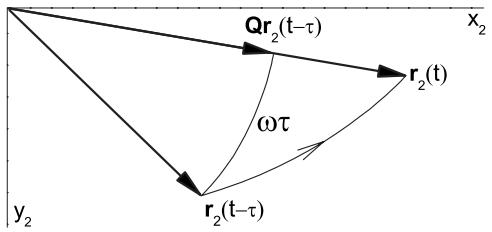

FIG. 1. Phase-lag compensation of the delayed vector $\mathbf{r}_2(t-\tau)$.

$$\mathbf{Q} = \begin{pmatrix} \cos\alpha & -\sin\alpha & 0 \\ \sin\alpha & \cos\alpha & 0 \\ 0 & 0 & 0 \end{pmatrix} \tag{4}$$

is a 3×3 matrix that projects the vector field onto the unstable (x,y) plane and rotates this projection by the angle $\alpha=\omega\tau$. Here ω is a frequency of the unstable spiral, which for the Rössler system is ≈ 1. The main advantage of such a choice consists in phase-lag compensation of the time-delay feedback term in Eq. (1b). When the system moves along the unstable spiral in the (x,y) plane, the vector $\mathbf{Qr}_2(t-\tau)$ is in-phase with the vector $\mathbf{r}_2(t)$ (cf. Fig. 1), and thus the term $\mathbf{Kr}_2(t-\tau)$ provides a correct negative feedback. We refer to this coupling law as a phase-lag compensating coupling (PLCC). In Fig. 2 we compare the effect of PLCC with the usual diagonal coupling, when $\mathbf{K}=k$ diag[1,1,1]. The time of reliable prediction for the PLCC is $\tau\approx 3.8$. It exceeds 4 times the maximum prediction time for the diagonal coupling. The characteristic period of chaotic oscillations for the Rössler system is ≈ 6. Thus our algorithm allows us to make prediction for more than a half of this period.

We stress that the PLCC enables forecasting of the *global* dynamics of the system, although the coupling matrix (4) takes into account only the *local* properties of the phase space. Indeed, the phase-lag compensation via rotation of the vector field is strongly valid only in the vicinity of the fixed point. It is notable that a similar rotation feedback gain has been recently used by Fiedler *et al.* [21] in a problem of the

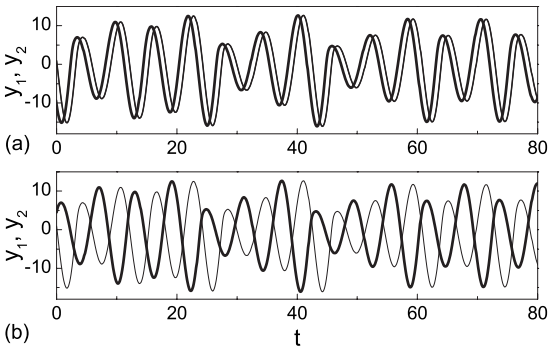

FIG. 2. Time series $y_1(t)$ of the master (thin line) and $y_2(t)$ of the slave (bold line) Rössler systems. (a) The diagonal coupling with $\mathbf{K}=0.36$ diag[1,1,1] and $\tau=0.9$. (b) The PLCC with $\mathbf{K}=0.18\mathbf{Q}$, $\omega=1$, and $\tau=3.6$. In both cases the coupling parameters are optimized in such a way as to attain the maximum stably anticipation time.

delayed feedback control [22] to overcome the so-called odd-number limitation.

We now consider a more precise and more general development of the above idea for any Rössler-type dynamical system. Suppose that a strange attractor of a 3D chaotic system $\dot{\mathbf{r}}=\mathbf{f}(\mathbf{r})$ originates from a saddle-focus fixed point $\mathbf{r}_0$ such that $\mathbf{f}(\mathbf{r}_0)=0$. Generally, the unstable and stable manifolds of the fixed point may have arbitrary orientations in the phase space. To design the coupling for this general case we first shift coordinates to the fixed point and rewrite the governing equation in the form $\dot{\mathbf{R}}=\mathbf{JR}+\mathbf{N}(\mathbf{R})$, where $\mathbf{J}=\partial\mathbf{f}/\partial\mathbf{r}|_{\mathbf{r}=\mathbf{r}_0}$ is the Jacobian matrix, $\mathbf{N}(\mathbf{R})=\mathbf{f}(\mathbf{r}_0+\mathbf{R})-\mathbf{JR}$ is a nonlinear function, and $\mathbf{R}=\mathbf{r}-\mathbf{r}_0$. Then Eq. (1b) for the slave system can be written as

$$\dot{\mathbf{R}}_2 = \mathbf{JR}_2 + \mathbf{N}(\mathbf{R}_2) + \mathbf{K}[\mathbf{R}_1 - \mathbf{R}_2(t-\tau)]. \tag{5}$$

According to our assumptions, the Jacobian $\mathbf{J}$ has a pair of complex-conjugate eigenvalues $\lambda_{1,2}=\gamma\pm i\omega$ with $\gamma>0$, corresponding to the 2D unstable spiral manifold, and a real negative eigenvalue λ_3, representing the stable 1D manifold. By a suitable change of variables, the Jacobian $\mathbf{J}$ can be transformed to Jordan normal form—that is,

$$\mathbf{E}^{-1}\mathbf{JE} = \begin{pmatrix} \gamma & -\omega & 0 \\ \omega & \gamma & 0 \\ 0 & 0 & \lambda_3 \end{pmatrix}, \tag{6}$$

where $\mathbf{E}$ is the matrix of eigenvectors of $\mathbf{J}$. This transformation orients the unstable 2D manifold towards the (x,y) plane and the stable manifold towards the z axes. After such a transformation we can apply the above theoretical arguments and use the coupling law $\mathbf{K}=k\mathbf{Q}$. This means that in the original (nontransformed) variables the coupling matrix has to be constructed as

$$\mathbf{K} = k\mathbf{EQE}^{-1}. \tag{7}$$

Equation (7) gives a general algorithm of coupling design for typical chaotic systems. Application of the general coupling law (7) to the Rössler system does not advance significantly the forecasting algorithm in comparison to the above-considered heuristic approach. This is because the Jacobian of the Rössler system is close to the Jordan normal form and the matrix $\mathbf{EQE}^{-1}$ does not differ significantly from the matrix $\mathbf{Q}$. Nevertheless, below we present the results of a linear stability analysis for the Rössler systems coupled by matrix (7).

The linear stability of the anticipating synchronization is determined by the variational equation

$$\delta\dot{\mathbf{r}}_2 = \left.\frac{\partial\mathbf{f}}{\partial\mathbf{r}_2}\right|_{\mathbf{r}_2=\mathbf{r}_1(t+\tau)} \delta\mathbf{r}_2 - \mathbf{K}\,\delta\mathbf{r}_2(t-\tau), \tag{8}$$

where $\delta\mathbf{r}_2=\mathbf{r}_2(t)-\mathbf{r}_1(t+\tau)$ is a transversal deviation from the synchronization manifold. The growth rates of this deviation define the transversal Lyapunov exponents. A necessary condition for the synchronized regime to be stable is that the maximum transversal Lyapunov exponent $\lambda_\perp$ be negative. In Fig. 3(a) we plot the dependence of $\lambda_\perp$ on the coupling strength k. There are two stability thresholds k_1 and k_2 for

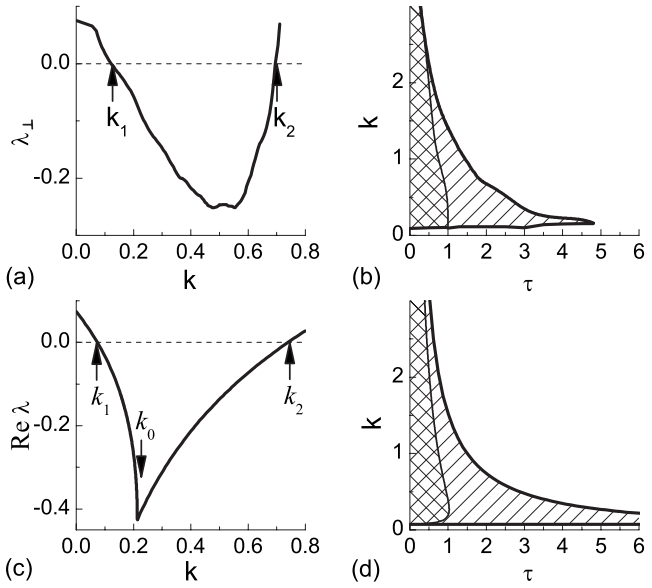

FIG. 3. (a) Maximum transversal Lyapunov exponent $\lambda_\perp$ vs k for the Rössler systems coupled by matrix (7) at $\tau=2$. (b) τ-k stability diagram for the Rössler systems. The bottom and upper bold curves show the dependences, respectively, of k_1 and k_2 thresholds on τ for PLCC. The region between these curves filled by right-tilted lines represent the stable synchronized state for PLCC. The thin curve bounds the synchronization region (filled by left-tilted lines) for diagonal coupling with $\mathbf{K}=k$ diag[1,1,1]. (c) and (d) The same as (a) and (b), respectively, but for the system (9). The parameters of the spiral are taken to be the same as the eigenvalues of the fixed point of the Rössler system—i.e., $\omega=0.997$ and $\gamma=0.074$. The boundaries of stability for PLCC in the (τ,k) plane are determined by $k_1=\gamma$ and $k_2(\Omega)=(\gamma^2+\Omega^2)^{1/2}$, $\tau(\Omega)=\arctan(\Omega/\gamma)/\Omega$, where $\Omega \in [0,\infty]$ is a parameter. The boundary of stability for diagonal coupling is defined by $\tau(\Omega)=\arctan[(\Omega-\omega)/\gamma]/\Omega$, $k(\Omega)=\gamma/\cos(\Omega\tau)$, $\Omega\in[\omega,\infty]$.

which $\lambda_\perp(k_1)=\lambda_\perp(k_2)=0$. The synchronized state is stable in the interval $k_1<k<k_2$ where $\lambda_\perp(k)<0$. In Fig. 3(b), we demonstrate the advantages of the PLCC over diagonal coupling by plotting the stability diagram in the plane of parameters (τ,k). The region of stability of the synchronized state for the PLCC is considerably larger than that for the diagonal coupling.

The above numerical results can be explained by a simple analytical model. If we suppose that the main contribution to the maximum Lyapunov exponent comes from system's motion along the unstable spiral, then it is reasonable to consider anticipating synchronization for the mere spirals. Specifically, assume that the dynamical system under consideration is described by two linear equations $\dot{x}=\gamma x-\omega y$ and $\dot{y}=\omega x+\gamma y$, which define an unstable spiral with positive increment γ and frequency ω. For the complex variable $Z=x+iy$, this system can be presented by a single equation $\dot{Z}=(\gamma+i\omega)Z$. Then equations for anticipating synchronization of two spirals take the form

$$\dot{Z}_1=(\gamma+i\omega)Z_1, \tag{9a}$$

$$\dot{Z}_2=(\gamma+i\omega)Z_2+ke^{i\alpha}[Z_1-Z_2(t-\tau)], \tag{9b}$$

where $ke^{i\alpha}$ is a complex coupling coefficient. By a suitable choice of phase α we can model both the PLCC ($\alpha=\omega\tau$) and diagonal coupling ($\alpha=0$). The solution of the master system is $Z_1=Z_0e^{(\gamma+i\omega)t}$, and the deviation $\delta Z_2=Z_2(t)-Z_0e^{(\gamma+i\omega)(t+\tau)}$ from the anticipated state satisfies $\delta\dot{Z}_2=(\gamma+i\omega)\delta Z_2-ke^{i\alpha}\delta Z_2(t-\tau)$. Substituting $\delta Z_2=Ce^{(\lambda+i\omega)t}$ we obtain the characteristic equation

$$\lambda=\gamma-ke^{i(\alpha-\omega\tau)}e^{-\lambda\tau}, \tag{10}$$

which defines the eigenvalues λ of the synchronized state in a rotating frame with frequency ω. For PLCC, $\alpha=\omega\tau$ and the solution of Eq. (10) is $\lambda=\gamma+W(-\tau ke^{-\gamma\tau})/\tau$, where $W(z)$ is the Lambert W function, satisfying by definition $W(z)e^{W(z)}=z$ [23]. The leading eigenvalue is determined by the principal branch of the Lambert function; its dependence on k, for the parameters γ and ω the same as for the Rössler system, is shown in Fig. 3(c). The minimal value of this dependence is $\lambda(k_0)=\gamma-1/\tau$, where $k_0=e^{\gamma\tau-1}/\tau$. The necessary condition for stability of the synchronized state is $\lambda(k_0)<0$ or $\tau<1/\gamma$. As expected from a general theory, the limit for the prediction horizon is determined by the inverse of the largest Lyapunov exponent, which for the spiral is $1/\gamma$. In Fig. 3(d) we compare stability regions in the (τ,k) plane for the PLCC ($\alpha=\omega\tau$) and diagonal coupling ($\alpha=0$). They are in approximate quantitative agreement with the corresponding regions of the Rössler system shown in Fig. 3(b). Thus the characteristic parameters of anticipating chaotic synchronization can be estimated analytically from the simple linear equations (9) that model local dynamics of the chaotic system close to the fixed point.

PLCC allows us to extend the prediction horizon not only for Rössler-type systems, but also for more complex double--

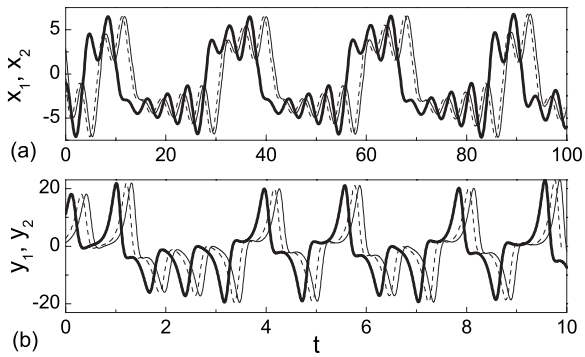

FIG. 4. Dynamics of the master (thin line) and the slave systems coupled by PLCC (bold line) and diagonal coupling (dashed line) for the Chua (a) and Lorenz (b) double-scroll attractors. (a) The parameters for PLCC are $k=0.18$, $\omega=1.5698$, and $\tau=3.3$ and for diagonal coupling $\mathbf{K}=0.3$ diag[1,1,1] and $\tau=0.5$. (b) The parameters for PLCC are $k=2.4$, $\omega=10.1945$, and $\tau=0.3$ and for diagonal coupling $\mathbf{K}=5$ diag[1,1,1] and $\tau=0.1$. The parameters are chosen in such a way as to attain the maximum stably anticipation time.

scroll attractors. A typical example of such a system is the Chua circuit [24] defined by the flow

$$\mathbf{f}(\mathbf{r}) = ([g(y-x) - i_N]/C_1, [g(x-y) + z]/C_2, -y/L), \quad (11)$$

where x, y, and z represent, respectively, the tension across two capacitors and the current through the inductor, and $i_N = m_0 x + 0.5(m_1 - m_0)(|x+B_p| - |x-B_p|)$ is a piecewise-linear function. We choose the parameters $C_1=0.1$, $C_2=1$, $L=1/5$, $m_0=-0.5$, $m_1=-0.8$, $B_p=1$, and $g=0.58$ such that the circuit operates in the double-scroll regime. The double-scroll attractor originates from two saddle-focus fixed points $\mathbf{r}_0^{\pm} = [\pm x_0, 0, \mp g x_0]$, where $x_0=(m_0-m_1)B_p/(g+m_0)$. These fixed points have identical eigenvalues and eigenvectors since their Jacobian matrices coincide. Therefore the same coupling matrix (7) is suited to both fixed points and we get correct phase-lag compensation when the trajectory twists along of one or other scroll of the strange attractor. In Fig. 4(a) we see that the maximum anticipation time obtained with the PLCC is 6.6 times larger as compared to the diagonal coupling.

Finally, in Fig. 4(b), we demonstrate advantages of the PLCC for the Lorenz system [25] given by

$$\mathbf{f}(\mathbf{r}) = (\sigma(y-x), rx - y - xz, xy - bz). \quad (12)$$

We set $\sigma=10$, $b=8/3$, and $r=28$. Here the saddle-focus fixed points responsible for a double-scroll behavior are $\mathbf{r}_0^{\pm} = [\pm x_0, \pm x_0, r-1]$, where $x_0=[b(r-1)]^{1/2}$. Now the Jacobians of the fixed points do not coincide $\mathbf{J}_+ \neq \mathbf{J}_-$ and we use two different coupling matrices depending on the proximity of the system state to a given fixed point. Specifically, we take $\mathbf{K}=k\mathbf{E}_+\mathbf{Q}\mathbf{E}_+^{-1}$ for $y_2>0$ and $\mathbf{K}=k\mathbf{E}_-\mathbf{Q}\mathbf{E}_-^{-1}$ for $y_2<0$, where $\mathbf{E}_+$ and $\mathbf{E}_-$ are the matrices of eigenvectors of $\mathbf{J}_+$ and $\mathbf{J}_-$, respectively. As a result, we gain a 3 times longer prediction time than for the diagonal coupling.

In summary, we have proposed an algorithm of coupling design for a long-term anticipating synchronization of chaos. The algorithm is based on phase-lag compensation in the time-delay feedback term of the slave system. The maximum prediction time attained with the single-slave system is comparable to characteristic time scales of chaotic oscillations. The algorithm can be used as a strategy for real-time forecasting of chaotic dynamics in many technical applications. We hope that our findings will stimulate the search for appropriate coupling laws in other problems of anticipating synchronization—e.g., to enhance the predictability of chaotic systems with unknown dynamical models [26] or excitable systems driven by random forcing [16,17].

[1] A. Pikovsky, M. Rosenblum, and J. Kurths, *Synchronization: A universal concept in nonlinear sciences* (Cambridge University Press, Cambridge, England, 2001).
[2] S. Boccaletti, J. Kurths, G. Osipov, D. L. Valladares, and C. S. Zhou, Phys. Rep. **366**, 1 (2002).
[3] V. S. Afraimovich, N. N. Verichev, and M. I. Rabinovich, Izv. Vyssh. Uchebn. Zaved., Radiofiz. **29**, 795 (1986).
[4] L. M. Pecora and T. L. Carroll, Phys. Rev. Lett. **64**, 821 (1990).
[5] N. F. Rulkov, M. M. Sushchik, L. S. Tsimring, and H. D. I. Abarbanel, Phys. Rev. E **51**, 980 (1995).
[6] M. G. Rosenblum, A. S. Pikovsky, and J. Kurths, Phys. Rev. Lett. **76**, 1804 (1996).
[7] R. Mainieri and J. Rehacek, Phys. Rev. Lett. **82**, 3042 (1999).
[8] M. G. Rosenblum, A. S. Pikovsky, and J. Kurths, Phys. Rev. Lett. **78**, 4193 (1997).
[9] H. U. Voss, Phys. Rev. E **61**, 5115 (2000).
[10] C. Masoller, Phys. Rev. Lett. **86**, 2782 (2001).
[11] O. Calvo, D. R. Chialvo, V. M. Eguíluz, C. Mirasso, and R. Toral, Chaos **14**, 7 (2004).
[12] M. Kostur, P. Hänggi, P. Talkner, and J. L. Mateos, Phys. Rev. E **72**, 036210 (2005).
[13] H. U. Voss, Int. J. Bifurcation Chaos Appl. Sci. Eng. **12**, 1619 (2002).
[14] S. Sivaprakasam, E. M. Shahverdiev, P. S. Spencer, and K. A. Shore, Phys. Rev. Lett. **87**, 154101 (2001).
[15] S. Tang and J. M. Liu, Phys. Rev. Lett. **90**, 194101 (2003).
[16] M. Ciszak, O. Calvo, C. Masoller, C. R. Mirasso, and R. Toral, Phys. Rev. Lett. **90**, 204102 (2003).
[17] M. Ciszak, F. Marino, R. Toral, and S. Balle, Phys. Rev. Lett. **93**, 114102 (2004).
[18] H. U. Voss, Phys. Rev. Lett. **87**, 014102 (2001).
[19] C. Mendoza, S. Boccaletti, and A. Politi, Phys. Rev. E **69**, 047202 (2004).
[20] O. E. Rössler, Phys. Lett. **57**, 397 (1976).
[21] B. Fiedler, V. Flunkert, M. Georgi, P. Hövel, and E. Schöll, Phys. Rev. Lett. **98**, 114101 (2007).
[22] K. Pyragas, Phys. Lett. A **170**, 421 (1992).
[23] R. M. Corless, G. H. Gonnet, D. E. G. Hare, D. J. Jeffrey, and D. E. Knuth, Adv. Comput. Math. **5**, 329 (1996).
[24] L. O. Chua, M. Komuro, and T. Matsumoto, IEEE Trans. Circuits Syst. **33**, 1072 (1986).
[25] E. N. Lorenz, J. Atmos. Sci. **20**, 130 (1963).
[26] M. Ciszak, J. M. Gutierrez, A. S. Cofino, C. Mirasso, R. Toral, L. Pesquera, and S. Ortin, Phys. Rev. E **72**, 046218 (2005).